JOURNAL OF MATERIALS SCIENCE 19 (1984) 3013–3020

Discontinuous precipitation in Cu–Mg alloys

H. TSUBAKINO
Department of Metallurgical Engineering, College of Engineering, University of Osaka Prefecture, Sakai, Osaka 591, Japan

R. NOZATO
Department of Materials Science, Himeji Institute of Technology, Himeji 671-22, Japan

The relation between discontinuous precipitation and continuous precipitation and the cell growth kinetics of the discontinuous precipitation in Cu–Mg alloys containing 2.0, 2.6 and 3.2 wt % Mg have been investigated, mainly by metallographic observation. The volume fraction of cells, the cell width and the interlamellar spacing have been determined by quantitative metallographic measurements. The cell growth rate decreases progressively with ageing time after the initial linear growth of the cells. This may be attributed to the influence of continuous precipitation on the cell growth. The volume fraction of the discontinuous precipitation cells, f, can be represented by the Johnson–Mehl equation: $f = 1 - \exp(-bt^n)$. The value of the parameter n is about 2 and is independent of both the ageing temperature and alloy composition in the ageing range where the cell growth rates are constants. Mass transport of magnesium during the linear growth of cells occurs by grain boundary diffusion in a Cu–Mg solid solution.

1. Introduction

Discontinuous precipitation has been observed in many alloy systems [1, 2]. Discontinuous precipitation, in general, occurs by a rapid nucleation at grain boundaries followed by a growth stage in which no further nucleation occurs.

The overall rate equation governing most discontinuous precipitation can be expressed in the Johnson–Mehl type of form [3]:

$$f = 1 - \exp(-bt^n) \quad (1)$$

where f is the volume fraction of the discontinuous precipitation cells, t is ageing time, and b and n are constants. However, a continuous precipitation also occurs simultaneously in many alloys and the continuous precipitation has an effect on the nucleation and growth of discontinuous precipitation [4–6]. The value of the time exponent n is independent of the ageing temperature and alloy composition when there is no continuous precipitation or the effect of continuous precipitation on discontinuous precipitation is negligible, as reported for Pb–Sn [7], Pb–Cd [8, 9], Cu–Cd [10] and Cu–Be [4, 5] alloys.

The only available study of the kinetics of discontinuous precipitation in Cu–Mg alloys is the work of Moisio and Mennerkoski [11]. They have reported that the value of n varies widely from 1 to 3 dependent on the ageing temperature and alloy composition. Although they also observed the continuous precipitation (the continuous precipitate is Cu_2Mg equilibrium phase [12]), they did not attempt to relate the experimentally observed variation of the value of n with the continuous precipitation occurring in the alloy. Furthermore, the cell growth kinetics in the alloy have not been previously reported.

In the present study, the relationship between the discontinuous precipitation and the continuous precipitation, and the kinetics of discontinuous precipitation have been investigated, mainly by metallographic measurements.

2. Experimental procedure

Three Cu–Mg alloys containing 2.0, 2.6 and 3.2 wt % magnesium were prepared from 99.99% Cu and 99.9% Mg. Copper was melted in a graphite crucible where the melt was protected against oxidation by the use of graphite powder. Magnesium wrapped in copper foil was added by using

0022–2461/84 $03.00 + .12

a graphite plunger. The melts were poured into an iron mould. Homogeneization was performed for 48 h at 983 K in an argon atmosphere. The ingots were hot- and cold-rolled to about 2×10^{-3} m in thickness. The chemical analysis of the magnesium content of the alloys was 2.01, 2.58 and 3.15 wt%. The mean grain sizes of the alloys were 2.5 to 3×10^{-4} m.

The specimens (10 mm × 10 mm × 2 mm) were solution annealed for one hour at 983 K in an argon atmosphere, quenched in iced water and subsequently aged isothermally. Ageing treatments were carried out in molten salt baths. Ageing temperatures were between 573 and 873 K.

The aged specimens were subjected to quantitative metallographic measurements with optical and electron microscopes. Replicas for electron microscopy were prepared by the two-stage germanium-shadowed technique.

The volume fraction of the discontinuous precipitation cells (f), the cell width (w) and interlamellar spacing within cells (l) were measured. f was determined by means of the lineal analysis method [13] in which the total scanning length was 9×10^{-2} m, w was taken as the largest distance perpendicular to the original grain boundaries from the advancing interface of cells and l was obtained from the Turnbull and Treaftis method [14].

In order to discover the relationship between the discontinuous precipitation and continuous precipitation, hardness measurements were performed at two different regions of the specimens, i.e. the grain boundary regions and grain centre regions, by using a microhardness tester.

3. Experimental results

3.1. Metallographic observations and hardness measurements

Typical microstructures of Cu–Mg alloys during ageing are shown in Fig. 1. During the initial ageing stages (Figs. 1a and b), discontinuous precipitation cells form at the original grain boundaries and advance into the grain interiors in which no precipitates can be found. As the ageing proceeds, continuous precipitation occurs in the grain interiors in which cells have not proceeded (Fig. 1c), and the cell growth rate seems to decrease at these ageing stages. Electron microscopy of surface replicas (Fig. 1d) indicates

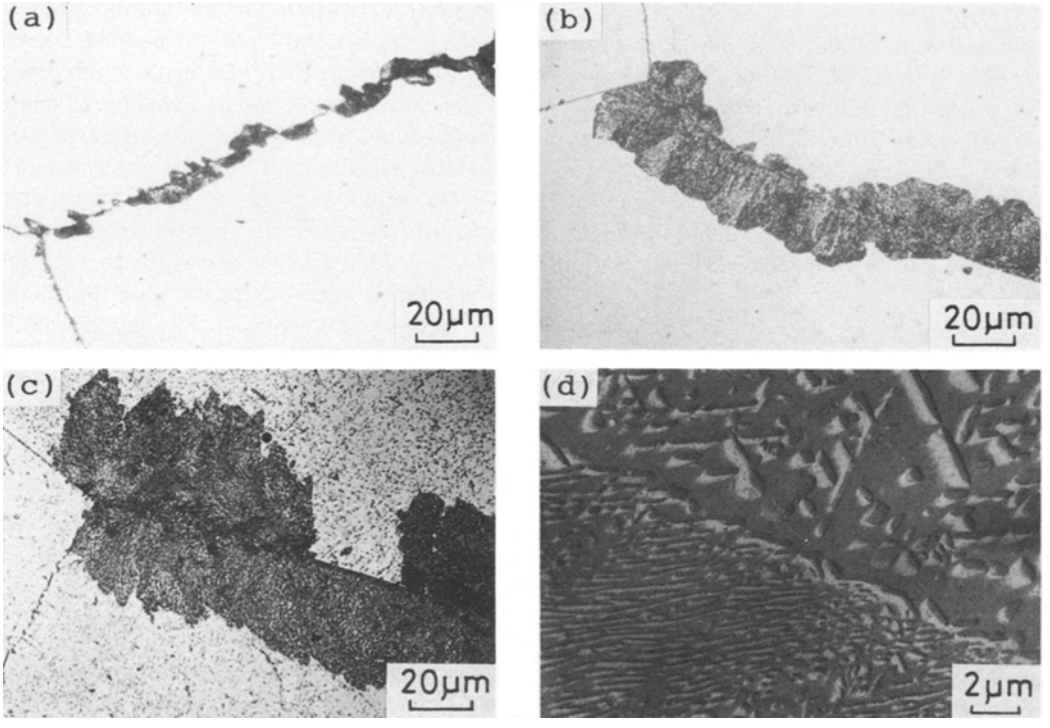

Figure 1 Typical microstructures of Cu–3.2 wt% Mg alloy. (a) Aged for 7.2×10^2 sec at 723 K, (b) aged for 1.8×10^3 sec at 723 K, (c) aged for 3.6×10^3 sec at 723 K and (d) aged for 9×10^4 sec at 723 K.

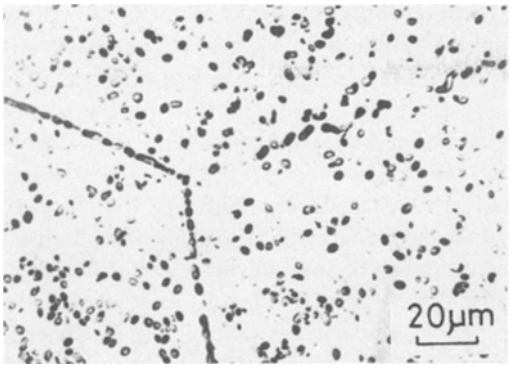

Figure 2 Microstructure of Cu–2.0 wt% Mg alloy aged for 1.66×10^5 sec at 823 K.

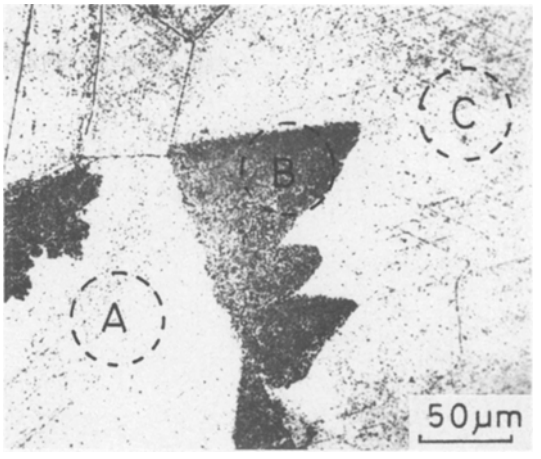

Figure 3 Microstructure of Cu–2.0 wt% Mg alloy aged for 1.88×10^5 sec at 673 K, with X-ray beams located at marked places.

that the cells consist of lamellar precipitates and these are finer than continuous precipitates. Fig. 1d further indicates that continuous precipitates locate along the advancing interface of the cells; this result suggests that the cell advance is suppressed by the continuous precipitate.

In the specimens aged at high temperatures closer to the solvus line, discontinuous precipitation cells are not observed (Fig. 2). This means that the continuous precipitation is favoured at relatively higher temperatures.

The circles in Fig. 3 indicate the areas irradiated by the X-ray beam used for obtaining back-reflection Laue photographs reproduced in Figs. 4a, b and c, respectively. The X-ray diffraction pattern from the area containing discontinuous precipitation has spots in exactly similar position as those from the adjacent grain. Therefore, the orientation of the depleted phase in the cell should be nearly identical with the neighbouring grain, i.e., the cell growth in this alloy is also associated with the migration of a grain boundary.

Fig. 5 shows the typical microhardness change (Vicker's hardness) as a function of the ageing time. The grain boundary regions start to harden corresponding to the appearance of the discontinuous precipitation cell, pass through a maximum value and then fall gradually. On the other hand, the grain interiors start to harden more slowly than the grain boundary regions. This difference in hardening response in the two regions is consistent with the results of metallographic observations. The maximum hardness in the grain interiors is lower than that in the grain boundary regions, which also corresponds to the metallographic observations, precipitate size, as shown in Fig. 1d.

3.2. Kinetics of discontinuous precipitation

The relation between the volume fraction of discontinuous precipitation (f) and ageing time (t) at various ageing temperatures in the three alloys showed sigmoidal curve behaviour. Using these

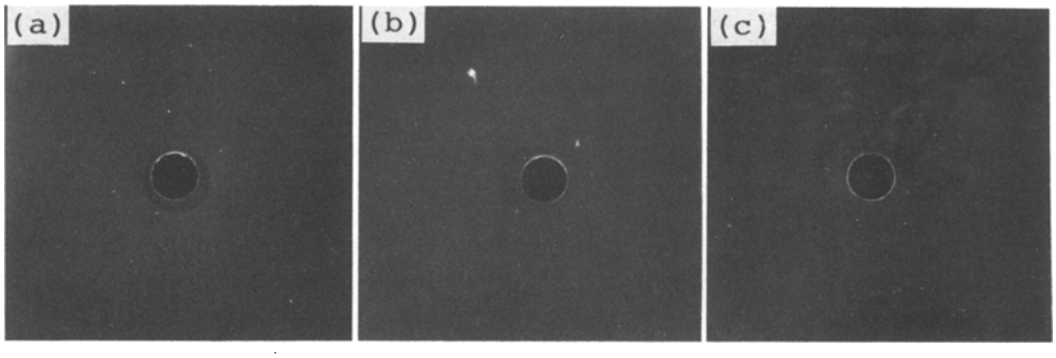

Figure 4 Back-reflection Laue patterns of areas marked in Fig. 3.

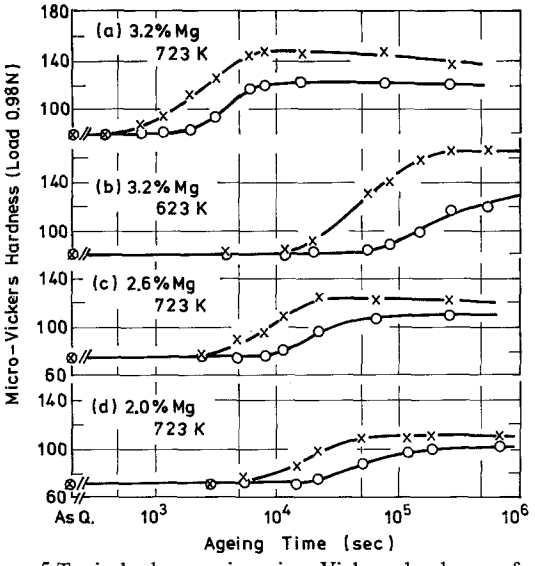

Figure 5 Typical changes in micro-Vickers hardness of Cu–Mg alloys. X: Grain boundary regions and ○: grain centre regions.

relations, log–log $\{1/(1-f)\}$ is plotted against $\log t$, as shown in Figs. 6 and 7. An approximately linear relationship is found at initial stages of ageing and the value of the time exponent "n" obtained from the slopes of these lines is about 2. This means that n is independent of ageing temperature and alloy composition. Figs. 6 and 7 further indicate that the plots deviate from the linear relationship and n decreases with ageing time during later stages of ageing.

3.3. Relationship between cell width and ageing time

The relationship between the cell width (w) and t at various ageing temperatures in Cu–3.2 wt% Mg alloy is shown in Fig. 8. The cell growth rate is given from the slope of these curves. The growth rate is linear at the initial stages of ageing and then decreases with t. The ageing time for the onset of the deviation from the linear relationship, denoted as t_d, are close to the ageing times when the grain interiors start hardening (Fig. 5). Therefore, the decrease in cell growth rate can be attributed to the occurrence of continuous precipitation.

The linear growth rate (G) is plotted against the ageing temperatures (T_A) in Fig. 9. Generally G increases with T_A but G's of 2.0 and 2.6 wt% Mg alloys show a maximum at the different temperatures ~ 720 and ~ 750 K, respectively.

3.4. Interlamellar spacing

Interlamellar spacings (l) obtained from the specimens aged for times less than t_d, is plotted against T_A in Fig. 10. All the alloys show a linear relationship. The temperatures (T_u) obtained by the extrapolation of these lines to the horizontal axis ($1/l = 0$) are plotted on the Cu–Mg equilibrium phase diagram in Fig. 11. Consistent with the metallographic observation (Fig. 2), they are the highest temperatures in which continuous precipitation occurs in a given alloy. The ratio of T_u to the solvus temperatures (T_m) for each alloy, T_u/T_m, was 0.96 to 0.98. These values are different from Böhm's ratio ($T_u/T_m = 0.8$) [15], but similar to the results on Cu–Sb [16], Cu–In [17] and Cu–Be [18] alloys.

4. Discussion

4.1. Kinetics of discontinuous precipitation

As shown in Figs. 6 and 7, the n-value was about 2 at the initial stages of ageing but decreased with t

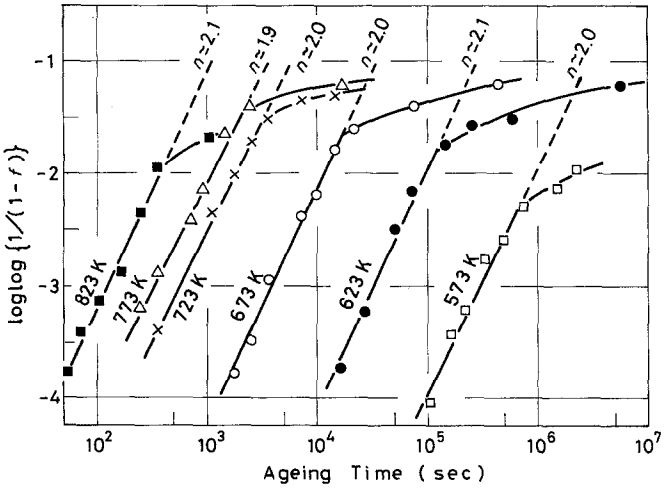

Figure 6 Plots of log–log $\{1/(1-f)\}$ against ageing time of Cu–3.2 wt% Mg alloy aged at various temperatures.

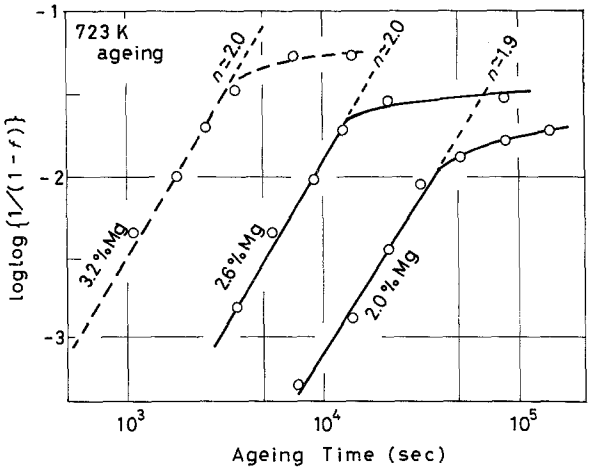

Figure 7 Plots of log–log $\{1/(1-f)\}$ against ageing time of various magnesium content alloys aged at 723 K.

in the later stages. The ageing times for the onset of the deviation of the n-value from 2 correspond well to the t_d's defined earlier. The decrease in the n-value, therefore, may be attributed to the decrease in the cell growth rate due to the effect of continuous precipitation on the cell growth. In this alloy system, the continuous precipitate is Cu_2Mg equilibrium phase [12]. The magnesium content in the matrix, which is closely related to the driving force for the cell growth, should decrease with the continuous precipitation. In addition, the advance of cells will be suppressed by the presence of continuous precipitates, as shown in Fig. 1d. Therefore, it can be concluded that the decrease in n is due to the occurrence of the continuous precipitation.

The n-value obtained from the linear relationship was independent of the ageing temperature (T_A) and alloy composition. These results are different from those of Moisio and Mannerkoski [11]. These investigators have shown that n varies widely with T_A and alloy composition. Their results show that n increases from 1 to 3 with the increase of T_A from 473 to 673 K and decreases from 3 to 1.5 with a further increase of T_A to 723 K in Cu–2.49 wt% Mg alloy. Furthermore, value of n at 673 K decreases from 3 to 1 with a decrease of magnesium content from 2.49 to 1.54 wt%. However, they did not pay attention to the possible relationship between the discontinuous precipitation and the continuous precipitation, as they measured f larger than 2%. But the measurements on f in this study have been taken with the specimens in much earlier stages of ageing

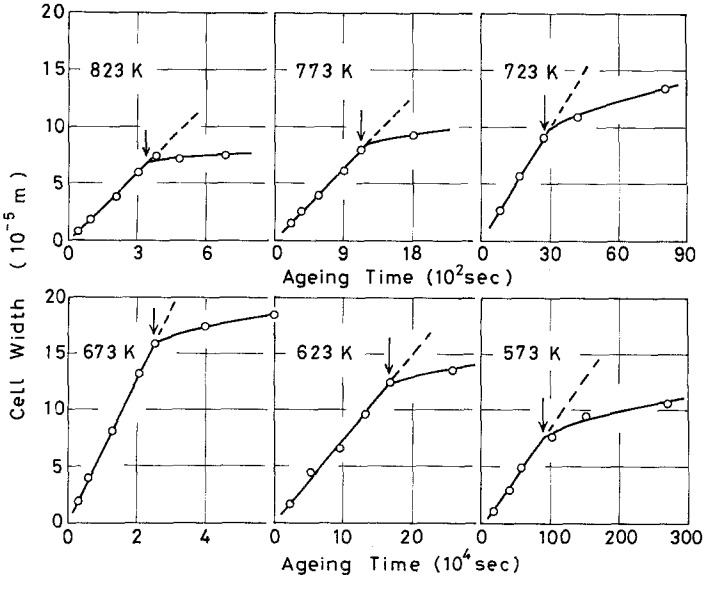

Figure 8 Dependence of cell width on ageing time of Cu–3.2 wt% Mg alloy aged at various temperatures. ↓: Time for beginning of a decrease in cell growth rate (t_d).

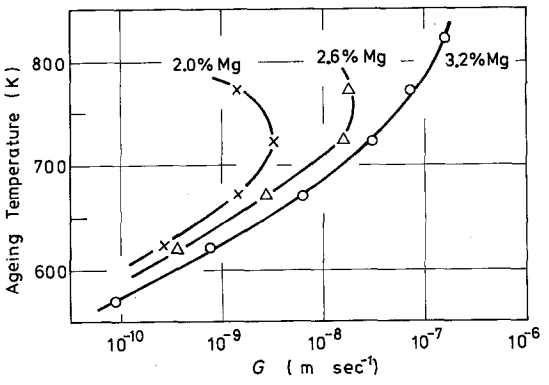

Figure 9 Dependence of the linear cell growth rates (G) on ageing temperature of various magnesium content alloys.

($f \geqslant 0.01\%$). It is difficult to compare directly these f-values with Moisio *et al.*'s data, because the magnesium content and grain size of alloys are different. Moreover, careful examination of Moisio *et al.*'s paper reveals that $n \simeq 1$ was obtained from the ageing stages where continuous precipitates can be observed in their micrograph. Therefore, their data might have been obtained from the later stages of ageing when a continuous precipitation has occurred.

In this study, f at t_d was different depending on T_A and magnesium content, as follows:

(i) f at t_d decreases as T_A increases from 773 to 823 K.

(ii) f at t_d decreases as T_A decreases from 723 to 573 K.

(iii) f at t_d decreases as magnesium content decreases.

This dependency of f was similar to that of w

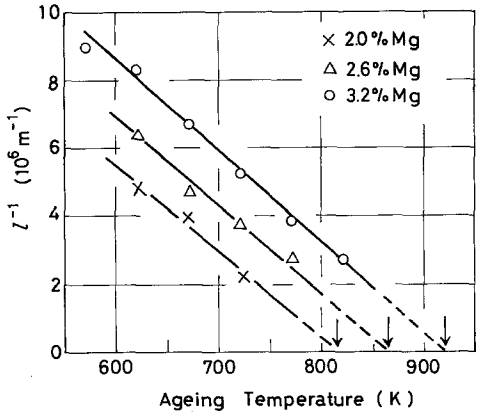

Figure 10 Dependence of reciprocal of interlamellar spacing (l^{-1}) on ageing temperature of various magnesium content alloys.

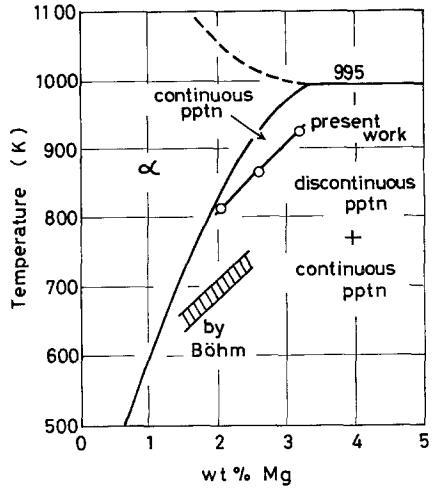

Figure 11 Part of Cu–Mg phase diagram and upper temperatures at which discontinuous precipitation occurs.

in this experiment. f depends on the number of cells per unit volume (N) and cell width (w). With increasing temperature or decreasing alloy composition, N should decrease because of the decrease of the degree of supersaturation. From metallographic measurements, it can be concluded that continuous precipitation is favoured at higher temperatures. Therefore, the dependence of f as described in (i) will be attributed to the decrease of w and N with increasing T_A. The last dependence (iii) will be attributed to the decrease of N, but with decrease of T_A, f at t_d decreases again (ii). The density of the continuous precipitates should increase as temperature decreases. Since the continuous precipitate in this alloy is the stable phase [12], it would be expected that the retarding effect of the continuous precipitate on cell growth may become greater as the temperature decreases and the effect will appear in the early ageing stage of continuous precipitation.

In this study, the value $n = 3$ which Moisio *et al.* obtained was not observed. This discrepancy cannot be explained, but their results of n on ageing at 673 K in Cu–2.49 wt% Mg alloy might have some uncertainty because of less data.

From the above, it can be concluded that n is independent of the ageing temperature and alloy composition in the ageing stages when a continuous precipitation has not occurred or the influence of the continuous precipitation on the cell growth is small and/or negligible.

Cahn [19] proposed that various n's are obtained depending on what the active growth sites are, assuming a sufficiently high nucleation rate of

cells, namely $n = 1, 2$ or 3 when the active growth site of cells is grain boundary surface, edge or corner, respectively. In this work, $n = 2$ was obtained. This implies that grain boundary edges are exhausted (covered with growing cells) at a stage early in the ageing and the transformation proceeds only by the growth of cells, which coincides well with the results of this experiment.

4.2. Cell growth kinetics

The cell growth rate G is given by Zener's equation (Equation 2) when the cell growth is controlled by volume diffusion mechanism [20]:

$$G = 2(X_0 - X_e)/X_0 \times D_v/l \qquad (2)$$

where D_v is the volume diffusion coefficient of solute atom, X_0 and X_e are the initial solute concentration and the equilibrium concentration of the depleted matrix, respectively, and l is the interlamellar spacing. The G's in Pb–1.5 wt % Cd alloy ($T_A \geqslant 343$ K) [9], Co–Ta [21] and Ta–Cr [22] alloys were represented by Equation 2. The G observed in this study was compared with the G estimated from Equation 2 by using the experimental l and D_v of the impurities in copper [23] because the D_v of magnesium in Cu–Mg solid solution was not available. The estimated G was much less than 10^{-3} of the observed G. Therefore, the cell growth rate cannot be represented by Equation 2 in the present case.

Turnbull proposed the following growth equation when cell growth is controlled by the grain boundary diffusion mechanism [24]:

$$G = 2(X_0 - X_e)/X_0 \times D_b\lambda/l^2 \qquad (3)$$

where D_b is the grain boundary diffusion coefficient and λ is the effective boundary thickness.

Aaronson *et al.* [25] modified the Turnbull equation as follows:

$$G = 4\lambda D_b/l^2 \qquad (4)$$

Cahn [26] proposed the cell growth equation assuming that the solute concentration of the depleted phase has not arrived at the equilibrium concentration.

The present experimental results were treated according to the above equations. However, due to the lack of any information about the degree of segregation in the depleted phase, Cahn's equation was not used.

D_b-values obtained by assuming $\lambda = 50$ nm from Equations 3 and 4, denoted as D_b^T and D_b^{MT}, respectively, are plotted against the reciprocal of T_A in Fig. 12. Plots obtained from each equation give approximately linear relationships which are independent of alloy composition, shown as follows:

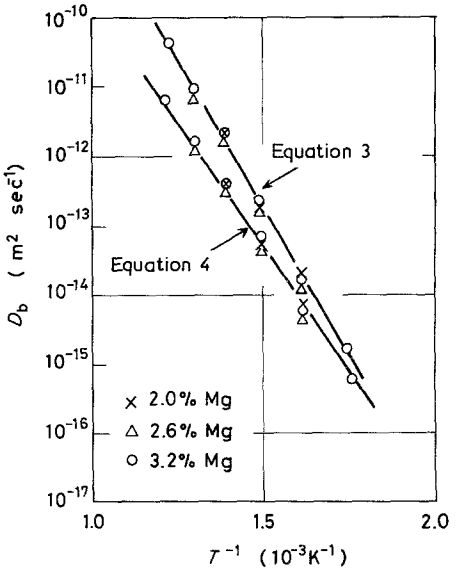

Figure 12 Arrhenius plots of grain boundary diffusitivities (D_b), evaluated from the Turnbull theory (Equation 3) and the modified Turnbull theory (Equation 4).

$$D_b^T = 0.89 \exp(-163000/RT) \text{m}^2 \text{ sec}^{-1} \qquad (5)$$

$$D_b^{MT} = 5.3 \times 10^{-3} \exp(-139000/RT) \text{m}^2 \text{ sec}^{-1} \qquad (6)$$

Since the data on D_b of magnesium in the Cu–Mg solid solution are not available, it is difficult to arrive at a conclusion about which of the equations used is a best approximation to the cell growth in Cu–Mg alloys. The activation energy (Q_b^T) obtained by using the Turnbull equation is considerably higher than Q_b^{MT}, and the ratio Q_b/Q_v is 0.7 to 0.9 from Equation 3 and 0.6 to 0.8 from Equation 4, where Q_v is the activation energy for the lattice diffusion of impurities in copper (176 to 234 kJ mol^{-1}) [23]. Furthermore, D_0 estimated from Equation 3 is widely different from the Zener range (10^{-5} to 10^{-3} m^2 sec^{-1}) [27]. Therefore, Equation 4 seems more reasonable to express the cell growth in this alloy, compared with Equation 3.

From the above, it can be concluded that the cell growth is controlled by the grain boundary diffusion of magnesium in Cu–Mg solid solution.

5. Conclusions

1. The decomposition of Cu_2Mg from supersaturated solid solutions of magnesium in copper during ageing is initiated by discontinuous precipitation and followed by continuous precipitation.

2. The cell growth rate decreases progressively with ageing time after the initial linear growth rate of cells. This can be attributed to the influence of the continuous precipitation on the cell growth.

3. The volume fraction of the discontinuous precipitation cells can be represented by the Johnson–Mehl equation: $f = 1 - \exp(-bt^n)$, where t is ageing time, and b and n are constants. The value of the parameter n is about 2, and is independent of both ageing temperature and alloy composition in the ageing range when cell growth rates are constants.

4. Interlamellar spacing increases with ageing temperature, whereas the linear cell growth rate first increases, passes through a maximum and then decreases.

5. Mass transport of magnesium during the linear growth of cells occurs by the grain boundary diffusion of magnesium in Cu–Mg solid solution.

Acknowledgements

The authors wish to thank Dr K. Chattopadhyay of the Indian Institute of Science for a number of comments on the original manuscript. A part of this work was originally published in Japanese in *J. Jpn. Inst. Met.* **47** (1983) 617.

References

1. R. WATANABE and S. KODA, *Bull. Jpn. Inst. Met.* **6** (1967) 435.
2. W. GUST, "Phase Transformations", Vol. 1, Ser. 3, No. 11 (Institute of Metallurgists, London, 1979) p. 27.
3. W. A. JOHNSON and R. F. MEHL, *Trans. AIME* **139** (1939) 415.
4. H. TSUBAKINO, R. NOZATO and H. HAGIWARA, *Trans. Jpn. Inst. Met.* **22** (1981) 153.
5. H. TSUBAKINO and R. NOZATO, *J. Jpn. Inst. Met.* **44** (1980) 131.
6. H. I. AARSONSON and J. B. CLARK, *Acta Metall.* **16** (1968) 845.
7. D. TURNBULL and H. N. TREAFTIS, *ibid.* **3** (1955) 43.
8. R. NOZATO, *J. Jpn. Inst. Met.* **24** (1960) 196.
9. R. NOZATO and H. TSUBAKINO, *ibid.* **37** (1973) 571.
10. M. SULONEN, *Ann. Acad. Soc. Fennicae, Ser. A* **6** (1957) 7.
11. T. MOISIO and M. MANNERKOSKI, *J. Inst. Met.* **95** (1967) 268.
12. S. HORI, S. SAJI and T. SEKIYA, *J. Jpn. Copper and Brass Res. Assoc.* **19** (1980) 115.
13. R. T. WOWARD and M. COHEN, *Trans. AIME* **172** (1947) 413.
14. D. TURNBULL and H. N. TREAFTIS, *Trans. Met. Soc. AIME* **212** (1958) 33.
15. H. BÖHM, *Z. Metallkde.* **52** (1961) 564.
16. B. PREDEL and W. GUST, *Met. Trans. A* **6A** (1975) 1237.
17. M. FREBEL, B. PREDEL and U. KLISA, *Z. Metallkde.* **65** (1974) 465.
18. H. TSUBAKINO and R. NOZATO, *J. Jpn. Inst. Met.* **43** (1979) 42.
19. J. W. CAHN, *Acta Metall.* **5** (1957) 169.
20. C. ZENER, *Trans. AIME* **167** (1946) 550.
21. M. KORCHYNSKY and R. W. FOUNTAIN, *Trans. Met. Soc. AIME* **215** (1959) 1033.
22. E. GEBHARDT and J. REXER, *Z. Metallkde.* **58** (1967) 611.
23. P. G. SHEWMON, "Diffusion in Solids" (McGraw-Hill, New York, 1963) p. 86.
24. D. TURNBULL, "Defects in Crystalline Solids", Report of Bristol Conference (Physics Society, London, 1954) p. 203.
25. H. I. AARONSON and Y. C. LIU, *Scripta Metall.* **2** (1968) 1.
26. J. W. CAHN, *Acta Metall.* **7** (1959) 18.
27. P. G. SHEWMON, "Diffusion in Solids" (McGraw-Hill, New York, 1963) p. 40.

Received 24 August
and accepted 29 November 1983